CO_2 Solubility in Organophosphate Physical Solvents Wherein Alkyl Groups Are Replaced with Poly(Ethylene Glycol) Groups

Robert L. Thompson,[1,2,*] Jeff Culp,[1,2] Surya P. Tiwari,[1,2] Wei Shi,[1,2] Nick Siefert,[1] and David Hopkinson[1]

[1] – U.S. Dept. of Energy, National Energy Technology Laboratory, 626 Cochran's Mill Rd., Pittsburgh, PA USA
[2] – Leidos Research Support Team, National Energy Technology Laboratory, 626 Cochrans Mill Rd., Pittsburgh, PA USA

* - corresponding author, e-mail address: robert.thompson@netl.doe.gov; tel: 412-386-4953

Abstract

Previous success in improving the CO_2 capacity of physical solvents for pre-combustion carbon capture by imparting poly(ethylene glycol) (PEG) functionality led us to compare tributyl phosphate (TBP), tri-isobutyl phosphate (T^iBP) and three analogous organophosphate solvents in which the length of PEG-substitution was varied. The PEG-substituted solvents proved to have acceptable densities and viscosities for the application of interest, but all three solvents showed poorer CO_2 absorption than TBP or T^iBP. Inclusion of hydrophilic PEG groups in solvents (**1**) – (**3**) also led to the undesired absorption of larger amounts of water from humidified N_2 compared to TBP and T^iBP. Computational studies of the analogous organophosphate solvents revealed that all solvents had the lowest partial negative charges, closest CO_2 interaction, and largest CO_2 interaction energy at the double bonded phosphoryl O atom. The fractional free volumes were computed and was found to be largest for T^iBP and grew progressively smaller as the length of the PEG group grew longer in solvents (**1**) – (**3**). Although introducing PEG groups to these molecules increased the number of interaction sites with CO_2, solvents (**1**) – (**3**) showed poorer CO_2 absorption than TBP and T^iBP due to their decreased solvent fractional free volume.

Introduction

Carbon capture and storage from fossil-based power generation is a critical component of realistic strategies for preventing a further rise in atmospheric CO_2 concentrations. However, capturing meaningful amounts of CO_2 using current technology could result in a prohibitive rise in the cost of electric power consumed. One strategy to minimize energy consumption and economic penalties is to exploit industrial streams in which CO_2 is already at high partial pressures, such as the syngas exiting coal gasifiers at integrated gasification combined cycle (IGCC) power plants. In these high-pressure CO_2-containing streams, one well-established approach to removing acid gases (CO_2 and H_2S) from the syngas stream is the use of physical solvents.[1]

The physical solvents used in pre-combustion capture of CO_2 from coal-gasified power plants are typically more effective at high pressures than chemical solvents.[2] Physical solvents that have been studied for CO_2 absorption include N-methyl-2-pyrrolidone (NMP - Purisol), propylene carbonate (Fluor solvent),[3] methanol (Rectisol),[4] and dimethyl ethers of polyethylene glycol (Selexol).[5,6]

One physical solvent that had been studied earlier, but was then seemingly neglected, is tributyl phosphate (TBP), originally identified in the Estasolvan process.[7] This solvent was used for natural gas purification and while it showed only moderate capacity to absorb CO_2, it was an excellent solvent for absorbing H_2S and SO_2.[8,9] The inclusion of etheric side chains in the form

of poly(ethylene glycol) (PEG) units of varying lengths has been shown to impart favorable gas absorption selectivities for CO_2 over CH_4 and N_2, while maintaining good CO_2 solubilities and other physical properties for imidazolium ionic liquids by Bara, et al.[10-12] Previously we reported on this approach as being successful for a novel liquid solvent, PEG-Siloxane-1, which is a hybrid solvent of PEG and poly(dimethyl siloxane) (PDMS),[13] and in other recent work.[14] This approach has greatly improved the CO_2 absorption capacity and CO_2/H_2 selectivity of these solvents and therefore was of interest to impart similar properties to TBP.

Research reported by Hess, et al.[15] has shown that organophosphates with PEG substituents are excellent liquid electrolyte media with useful properties including high boiling points and low viscosities, which also render them excellent candidates as CO_2 solvents. They reported the synthesis[16,17] of two symmetrical organophosphates from 2-methyoxyethan-1-ol and diethylene glycol, monomethyl ether, respectively, which we identified for study.

In this work we report the synthesis of these two products, which we refer to as $OP(1PEG)_3$ (**1** - tris(2-methoxyethyl) phosphate) and $OP(2PEG)_3$ (**2** - tris(2-(2-methoxyethoxy)ethyl) phosphate), as well as a third homologous product $OP(3PEG)_3$ (**3** - tris(2-(2-(2-methoxyethoxy)ethoxy)ethyl) phosphate) prepared using triethylene glycol, monomethyl ether. Herein, we report the physical properties, water absorption, thermal properties, and CO_2 absorption behavior of these three solvents and use computational results to describe their performance in comparison to TBP and its structural isomer tri-isobutyl phosphate (T^iBP).

Experimental

Syntheses

The preparation of the solvents discussed in this work were accomplished by way of a reaction between $POCl_3$ and an excess of alcohol catalyzed by 4-dimethylaminopyridine in dichloromethane (DCM); all reagents were used as received from Sigma Aldrich. The method of preparation of these compounds was derived from reactions reported by Hess, et al.[15-17] The solvents prepared in this work are shown in Figure 1. Three symmetrical solvents with different lengths of PEG-substituted side-chains were prepared, with their physical properties listed in Table 1 along with TBP and T^iBP.

Synthesis of tris(2-methoxyethyl) phosphate (**1**): A 500 mL round bottomed flask was charged with 2-methoxyethan-1-ol (62.3 g, 819 mmol, 4.16 equiv.), triethylamine (85.9 g, 849 mmol, 4.32 eq), and 4-dimethylaminopyridine (2.12 g, 17.4 mmol, 0.10 eq) dissolved in 200 mL DCM. The resultant homogeneous solution was cooled to 0°C in an ice bath and slowly treated drop-wise with phosphorus oxychloride (30.2 g, 197 mmol, 1 eq) dissolved in 100 mL DCM. The rate of dropping was controlled to occur over 60 min time with the temperature maintained around 0°C during which the clear reaction solution eventually became cloudy white. The resultant solution was left to stir at room temperature overnight. This solution was filtered to remove triethylamine hydrochloride, and the yellow DCM solution was washed twice with 300 mL 5% HCl and then 400 mL water. The organic layer was isolated and evaporated to give an off-white liquid, which was vacuum distilled to give a clear colorless liquid. ^{1}H NMR ($CDCl_3$): δ ppm 4.11 (m, $OC\underline{H}_2CH_2O$, 6H), 3.52 (m, $OCH_2C\underline{H}_2O$, 6H), 3.30 (m, OCH_3, 9H). ^{13}C NMR ($CDCl_3$): δ ppm 71.0 (d, 3C), 66.4 (d, 3C), 70.6 (s, 3C), 58.6 (s, 3C). ^{31}P NMR ($CDCl_3$): δ ppm -0.92. ESI MS: calc'd for $C_9H_{22}O_7P$

$(M+H)^+$ 273.23398, found 273.10826; calc'd for $C_9H_{21}NaO_7P$ $(M+Na)^+$ 295.22182, found 295.09046.

Synthesis of tris(2-(2-methoxyethoxy)ethyl) phosphate (**2**): A method similar to that described for (**1**) was employed using diethylene glycol, monomethyl ether (130 g, 1082 mmol, 4.04 equiv.), triethylamine (114 g, 1127 mmol, 4.20 eq), and 4-dimethylaminopyridine (2.62 g, 21.4 mmol, 0.08 eq) dissolved in 250 mL DCM and phosphorus oxychloride (41.1 g, 268 mmol, 1 eq) dissolved in 100 mL DCM. The crude product was vacuum distilled to give a clear colorless liquid. ^{1}H NMR ($CDCl_3$): δ ppm 4.10 (m, $OC\underline{H}_2CH_2O$, 6H), 3.61 (m, $OCH_2C\underline{H}_2O$, 6H), 3.54 (m, $OC\underline{H}_2CH_2OMe$, 6H), 3.43 (m, $OCH_2C\underline{H}_2OMe$, 6H), 3.26 (m, OCH_3, 9H). ^{13}C NMR ($CDCl_3$): δ ppm 71.6 (s, 3C), 70.2 (s, 3C), 71.6 (s, 3C), 70.2 (s, 3C), 69.7 (d, 1C), 66.4 (d, 3C), 58.7 (s, 3C). ^{31}P NMR ($CDCl_3$): δ ppm -1.13. ESI MS: calc'd for $C_{15}H_{34}O_{10}P$ $(M+H)^+$ 405.39756, found 405.18692; calc'd for $C_{15}H_{33}NaO_{10}P$ $(M+Na)^+$ 427.37950, found 427.16957.

Synthesis of tris(2-(2-(2-methoxyethoxy)ethoxy)ethyl) phosphate (**3**): A method similar to that described for (**1**) was employed using triethylene glycol, monomethyl ether (129 g, 783 mmol, 4.00 equiv.), triethylamine (84.3 g, 828 mmol, 4.23 eq), and 4-dimethylaminopyridine (2.06 g, 18.6 mmol, 0.09 eq) dissolved in 250 mL DCM and phosphorus oxychloride (30.1 g, 196 mmol, 1 eq) dissolved in 100 mL DCM. The crude product was vacuum distilled to give a clear colorless liquid. ^{1}H NMR ($CDCl_3$): δ ppm 4.11 (m, $OC\underline{H}_2CH_2O$, 6H), 3.62-3.54 (br m, $OC\underline{H}_2C\underline{H}_2O$, 24H), 3.54 (m, $OCH_2C\underline{H}_2OMe$, 6H), 3.29 (m, OCH_3, 9H). ^{13}C NMR ($CDCl_3$): δ ppm 71.7 (s, 3C), 70.2 (s, 3C), 70.4 (s, 6C), 70.3 (s, 3C), 69.7 (d, 3C), 66.5 (d, 3C), 58.7 (s, 3C). ^{31}P NMR ($CDCl_3$): δ ppm -1.05. ESI MS: calc'd for $C_{21}H_{49}NO_{13}P$ $(M+NH_4)^+$ 554.58178, found 554.29290; calc'd for $C_{21}H_{45}NaO_{13}P$ $(M+Na)^+$ 559.53718, found 559.24831.

Synthesis of T^{i}BP: A method similar to that described for (**1**) was employed using isobutyl alcohol (85.0 g, 1146 mmol, 4.27 equiv.), triethylamine (115 g, 1137 mmol, 4.24 eq), and 4-dimethylaminopyridine (2.58 g, 21.1 mmol, 0.08 eq) dissolved in 250 mL DCM and phosphorus oxychloride (41.1 g, 268 mmol, 1 eq) dissolved in 100 mL DCM. The crude product was vacuum distilled to give a clear colorless liquid. ^{1}H NMR ($CDCl_3$): δ ppm 3.72 (dt, $OC\underline{H}_2CH$, 6H), 1.88 (m, $CH_2C\underline{H}(CH_3)_2$, 3H), 0.87 (d, $CH(C\underline{H}_3)_2$, 18H). ^{13}C NMR ($CDCl_3$): δ ppm 73.3 (d, 3C, $O\underline{C}H_2CH$), 28.9 (d, 3C, $CH_2\underline{C}H(CH_3)_2$), 18.5 (s, 6C, $CH(\underline{C}H_3)_2$). ^{31}P NMR ($CDCl_3$): δ ppm -0.97. ESI MS: calc'd for $C_{12}H_{28}O_4P$ $(M+H)^+$ 267.17197, found 267.17240; calc'd for $C_{12}H_{27}NaO_4P$ $(M+Na)^+$ 289.15447, found 289.15400.

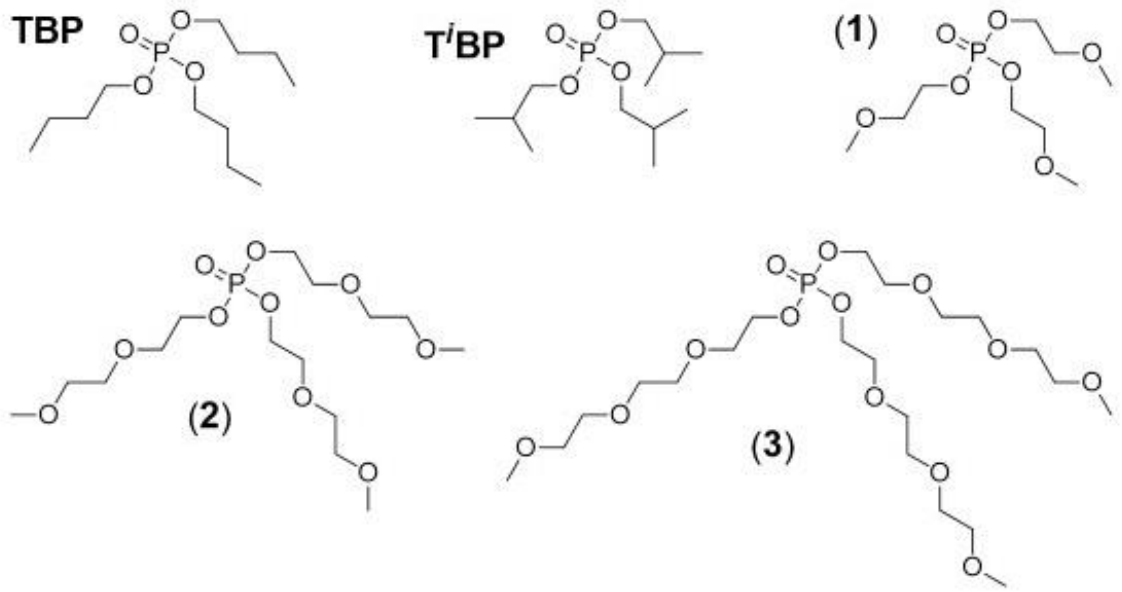

Figure 1. Molecular structures of TBP, T^{i}BP, and the three PEG-solvents prepared in this study: $OP(1PEG)_3$ (**1**), $OP(2PEG)_3$ (**2**), and $OP(3PEG)_3$ (**3**).

Instrumentation

Density measurements were completed on a Rudolph Research Analytical DDM 2911 automatic density meter at 25°C; all samples were measured with five replicates and the average density was reported. Viscosity measurements were performed on a Rheosense model μVisc micro-viscometer outfitted with a temperature controller set to 25°C; all samples were measured with five replicates and the average viscosity was reported. Moisture content was determined using a Metrohm Titrando Karl Fisher titration system at 120°C using 50 mL/min N_2 gas flow in oven mode; all samples were measured as three replicates and the average moisture content was reported.

TGA analyses were collected on a TA Instruments SDT-Q600 using 50 mL/min air as a sweep gas. ESI mass spectra were collected on dilute acetonitrile solutions using an Agilent 6520 QTOF LC-MS in positive ion mode. NMR data were collected on a Bruker Avance III 400 MHz spectrometer using a 5mm BBFO+ probe. All ^{1}H and ^{13}C NMR spectra were referenced to their respective solvent resonances.

Gas Absorption Experiments

Gravimetric CO_2 adsorption measurements were conducted on a Hiden IGA-001 microbalance. Samples (30-50 mg) were activated by purging with CO_2 at 70 mbar at 40°C until the sample weight stabilized. Isotherms were then measured under flowing CO_2 regulated by a mass flow controller and back pressure regulator. Equilibrium was determined at each pressure step using an internal fitting algorithm in the instrument control software. Buoyancy corrections were then applied to the final equilibrium weights using known densities of all components in the sample and counter weight chambers from gas densities calculated using REFPROP software from NIST. An additional minor correction (<5% of the adsorbed mass at 18 bar) was also applied to the final equilibrium sample mass at each pressure point to account for the small change in buoyancy force which results from volume expansion of the solvent during CO_2 adsorption.[18,19] The

volume expansion of the solvent was estimated from the mole fraction of CO_2 adsorbed using the molar volume of liquid CO_2 at 25°C (density of 0.7105 g/mL, 16.15 mol/L). Shiflett and Yokozeki employed a similar system to measure equilibrium CO_2 absorption in ionic liquids and estimated the relative uncertainty in CO_2 pressure to be 0.008 bar and in mole fraction CO_2 solubility to be less than 0.006.[20]

Water vapor adsorption measurements were conducted using an inline humidifier which was held at 23°C with a sample temperature of 25°C with N2 as the carrier gas. The relative humidity in the gas stream was controlled by blending dry N_2 with humidified N_2 prior to entering the sample chamber with the gas ratios set using mass flow controllers. Relative humidity in the sample chamber was then calculated from the sample chamber temperature and vapor pressure of water in the humidifier assuming complete saturation of the carrier gas. Final equilibrium loading of water vapor in the sample was determined by fitting the water adsorbed sample mass to an asymptotic model using OriginPro® (v 9.1) curve fitting software.

Computational Details

Ab initio gas phase calculations were performed to calculate the charges on each atom of the solvents and their interaction with CO_2. For each molecule, the geometry optimization was performed by using B3LYP/6-311++g(d,p) followed by charge calculations by using the CHELPG protocol.[21] The CO_2-molecule dimer was also optimized by using B3LYP/6-311++g(d,p) followed by a single point energy calculation at the MP2/cc-pVTZ level of theory to obtain CO_2 interaction with each molecule. To account for the basis set superposition error, we have used counterpoise corrections in both geometry optimization, frequency, and single point calculations for dimer computations. More calculation details were described in our previous work.[22,23] All ab initio calculations were performed by using the Gaussian 09 program.[24] All fractional free volume calculations were calculated by using a modified Bondi method,[25] which has been implemented in an in-house software package at NETL. We have reported further details on this method in our previous work.[14]

Results and Discussion

Physical Properties

Physical properties for all solvents studied are listed in Table 1. The density of TBP is slightly higher than T^{i}BP due to the presence of branched alkyl groups in the latter. The solvent density increases by 15% going from TBP to OP(1PEG)$_3$ (**1**); the densities then decrease slightly with the addition of increasingly longer PEG arms in (**2**) and (**3**). The viscosity of TBP is slightly lower than T^{i}BP and the viscosity of (**1**) was roughly double that of TBP, with viscosity increasing by a factor of two with each addition of increasingly longer PEG arms. The water content after drying for all molecules was consistently low, despite having been thoroughly water-washed; again, the water content increased slightly with the addition of increasingly longer PEG arms due to the presence of additional hydrophilic ether groups.

Table 1. Physical properties of PEG-substituted organophosphate solvents prepared.

product	FW, g/mol	density, g/mL at 25°C	viscosity, cP at 25°C	H_2O content, ppm
TBP	266.31	0.9728	3.84 ± 0.06	926
T^{i}BP	266.31	0.9618	4.75 ± 0.02	2202
OP(1PEG)$_3$ (**1**)	272.23	1.161	7.89 ± 0.04	1143
OP(2PEG)$_3$ (**2**)	404.39	1.149	18.9 ± 0.08	3352
OP(3PEG)$_3$ (**3**)	536.55	1.143	34.3 ± 0.48	3507

Spectroscopic Properties

The FTIR spectra of all four phosphate molecules were recorded and the frequency for phosphoryl group vibration was observed to shift slightly upwards as the length of the substituent groups increased (Table 2). This is consistent with results reported by Wagner, who related this trend to decreasing O-P bond order as the electronegativity of the ester group increases.[26] The presence of more O atoms in the ester groups withdraws electrons away from the phosphorus atom, which compensates by increasing the bond order in the phosphoryl π-bond. The downward shift of 5 cm^{-1} going from TBP to T^{i}BP suggests that the branched butyl groups are slightly more electron donating than linear groups, leading to a small decrease in P=O bond order.

Table 2. Spectroscopic properties of PEG-substituted organophosphate solvents prepared.

product	FTIR ν(O=P), cm^{-1}	^{31}P NMR δ, ppm in $CDCl_3$
TBP	1263	-0.72
T^{i}BP	1258	-0.97
OP(1PEG)$_3$ (**1**)	1263	-0.92
OP(2PEG)$_3$ (**2**)	1269	-1.13
OP(3PEG)$_3$ (**3**)	1272	-1.05

The ^{31}P NMR spectra for all four phosphate molecules were also noted, and the chemical shifts tended to shift upfield as the length of the substituent groups increased (also Table 2). This is also consistent with results reported by Gorenstein, who related this trend to increasing O-P-O bond angles in phosphate esters.[27,28] Substituents with greater steric bulk force themselves further apart, leading to larger O-P-O bond angles, which more effectively shields the ^{31}P nucleus.

CO_2 Absorption

The PEG-substituted solvents prepared in this work, TBP, and T^{i}BP were tested for CO_2 absorption at 25 and 40°C, using CO_2 pressures from 0 to 20 bar on the Hiden microbalance. Plots of moles of CO_2 dissolved per liter versus CO_2 pressure are illustrated in Fig. 2, with the linear fit for the highest slope (T^{i}BP at both temperatures) shown by a dashed line. Higher capacity for CO_2 absorption is reflected in larger slopes for the linear fit for these plots. The slope and correlation coefficient for each solvent at both temperatures are listed in Table 3. These plots were all linear ($r^2 \geq 0.997$) throughout the pressure ranges tested (0 to 10 bar).

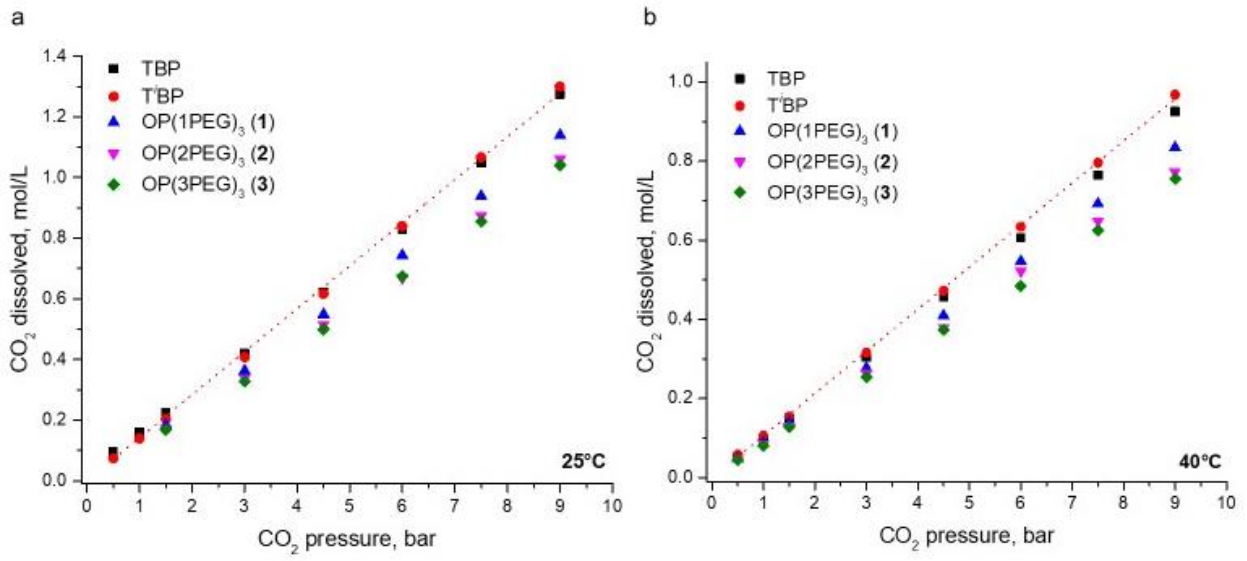

Figure 2. CO_2 absorption results measured by gravimetric Hiden microbalance at (a) 25°C and (b) 40°C for (**1**) - (**3**), TBP, and T^{i}BP.

Table 3. Comparison of CO_2 absorption plot linear fit slopes from gravimetric Hiden microbalance data and correlation coefficients achieved by TBP, T^{i}BP, and PEG-substituted organophosphate solvents at 25 and 40°C.

25°C data	**linear fit slope, mol/L bar**	**normalized slope[a]**	**r^2**
TBP[a]	0.1404	1.000	0.9987
T^{i}BP	0.1419	1.011	0.9989
OP(1PEG)$_3$ (**1**)	0.1250	0.890	0.9991
OP(2PEG)$_3$ (**2**)	0.1158	0.825	0.9978
OP(3PEG)$_3$ (**3**)	0.1138	0.811	0.9986

40°C data	**linear fit slope, mol/L bar**	**normalized slope[a]**	**r^2**
TBP[a]	0.1021	1.000	0.9998
T^{i}BP	0.1065	1.043	0.9997
OP(1PEG)$_3$ (**1**)	0.0922	0.903	0.9998
OP(2PEG)$_3$ (**2**)	0.0862	0.844	0.9998
OP(3PEG)$_3$ (**3**)	0.0832	0.815	0.9994

It was observed that CO_2 was most soluble in T^{i}BP at both temperatures. The CO_2 solubility decreased slightly going from T^{i}BP to TBP and decreased more significantly going from TBP to (**1**). The CO_2 solubility continued decreasing as the PEG arm grew longer for (**2**) and (**3**), with CO_2 absorption decreasing by as much as 10% for (**3**) at both temperatures. We have observed similar CO_2 absorption results when varying the PEG arm lengths in hybrid PEG/siloxane CO_2 solvents, where shorter PEG substituents tended to have higher CO_2 absorption.[13] But unlike those hybrid solvents, the inclusion of etheric groups failed to improve CO_2 uptake.

Absorption of Moisture

TBP and solvents (**1**) through (**3**) were exposed to moisture over a two-week period and the change in sample weight and water content was determined. An acrylic desiccator cabinet had two holes drilled into it on opposite sides and was fitted with plastic hose barbs. The cabinet was then purged with N_2 flowing through a gas bottle filled with water. The cabinet was able to maintain a relative humidity of around 80% under these conditions, as measured by a Dwyer Series 485 digital hygrometer. Glass vials were loaded with 1 g each of solvent, weighed, and stored with their caps off inside the humidification chamber. The weights were recorded once during the two-week test span and at the end of the experiment; the water content was determined by Karl Fisher titration before and after the two-week span.

Figure 3 shows the change in mole % water for TBP and (**1**) – (**3**), where the percentages have been normalized to the starting water content of the solvents. As the lengths of the PEG-substituents increases, the mole % water also increases steadily. The increase in mole % water exceeds three orders of magnitude for (**3**). The amount of water measured by Karl Fisher titration after humidification was consistent for all three PEG-substituted solvents at 40 wt % after two weeks exposure. The tendency of etheric groups to increase the hydrophilic character of molecules has been documented by Menger and Chlebowski, who reported that etheric surfactants show less tendency to self-aggregate and are less likely to adsorb onto hydrophobic surfaces than similar surfactants lacking ether groups.[29]

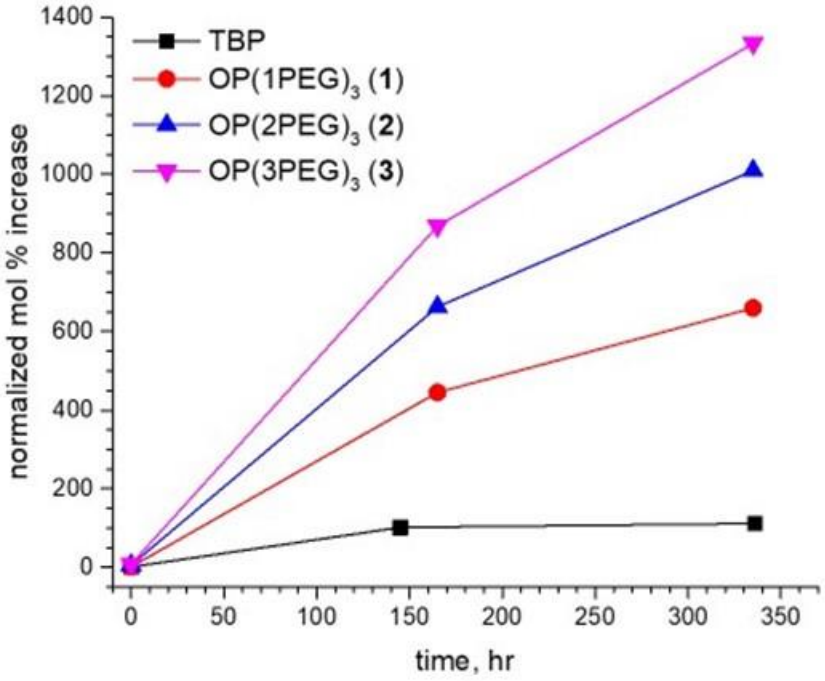

Figure 3. Plot of change in mole % water versus time spent in the humidification chamber for (**1**) - (**3**), and TBP.

TBP, T^{i}BP, and the PEG-substituted solvents prepared in this work were also tested for water absorption on the Hiden microbalance using humidified N_2. Plots of moles of H_2O absorbed per liter versus relative humidity are illustrated in Figure 4. TBP and T^{i}BP were observed to absorb nearly identical amounts of water, taking up only 2 mol/L at 90% relative humidity. The PEG-

substituted solvents were observed to take up nearly identical amounts of water under these conditions, at levels more than 4 times larger than TBP or T^{i}BP. It is interesting that (**1**) – (**3**) show an exponential-type increase in water absorption with increasing humidity, while TBP and T^{i}BP do not. Increasing numbers of etheric O atoms provide more water interaction sites in solvents (**1**) – (**3**). Thus, both the CO_2 and H_2O absorption properties of these functionalized TBP analogues become less favorable upon inclusion of etheric groups.

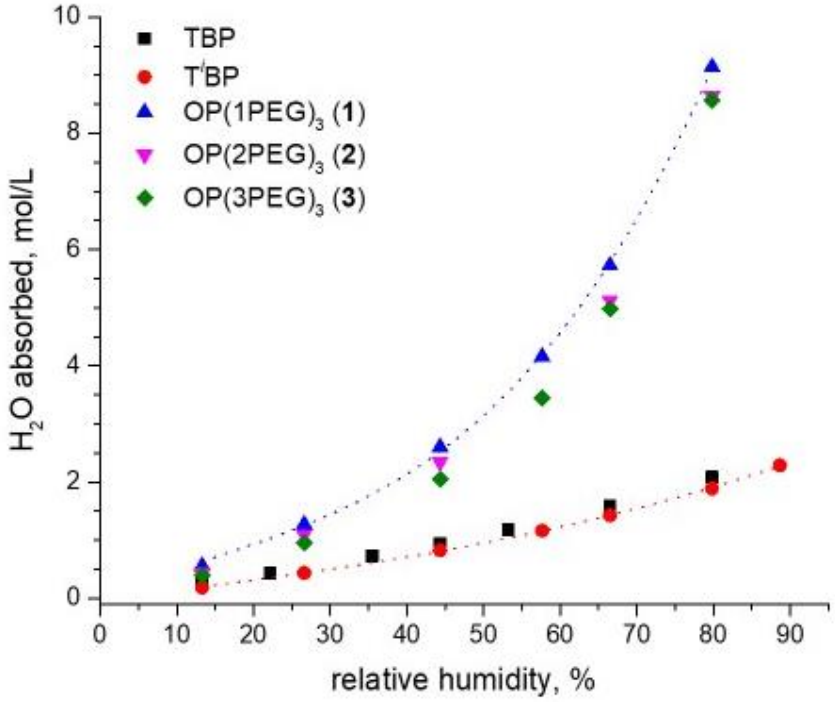

Figure 4. Water absorption results from humidified N_2 as measured by gravimetric Hiden microbalance at 25°C for (**1**) - (**3**), TBP, and T^{i}BP.

Thermal Properties

All five solvents were studied by thermal gravimetric analysis (TGA) to determine the thermal stability of the various conformations. A small aliquot of each molecule (ca. 15-20 mg) was loaded into an alumina TGA pan and temperature was ramped to 750°C at 10°C/min under 100 mL/min air while the sample mass was recorded. The first derivative maximum (T_{dec}) for each solvent was taken as a measure of the point at which the maximum rate of sample loss was experienced. The results are listed in Table 4, which shows that the decomposition temperature increases with increasing molecular weight for all four solvents.

Table 4. Thermal properties of TBP and PEG-substituted organophosphate solvents.

product	T_{dec}, °C	wt% lost/hr at 80°C	wt% lost/day at 80°C
TBP	214	9.18	>100
T^{i}BP	157	19.5	>100
OP(1PEG)$_3$ (**1**)	235	2.09	50.1
OP(2PEG)$_3$ (**2**)	294	0.504	12.1
OP(3PEG)$_3$ (**3**)	319	0.324	7.78

The solvents were also tested for longer term thermal stability (as an approximation of their tendency to evaporate) by exposing aliquots to 80°C temperatures for two days under 50 mL/min air flow to estimate the amount of weight loss to be expected due to volatility. These results are also listed in Table 4, and the results show that the weight lost decreases with increasing molecular weight, as shown in Figure 5. Both (**2**) and (**3**) lost approximately 10 wt% over the two-day span, whereas (**1**) lost almost 90 wt%, and both TBP and T^{i}BP had completely evaporated during this time. Unlike the CO_2 and H_2O absorption properties, the tendency of these functionalized TBP analogues to evaporate improved upon inclusion of etheric groups.

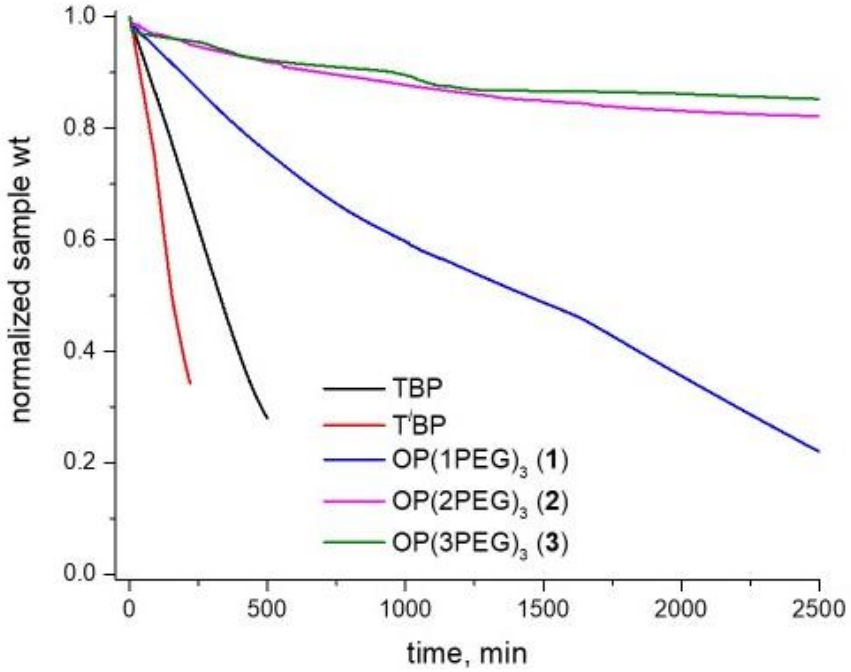

Figure 5. Evaporation of (**1**) - (**3**), TBP, and T^{i}BP in 50 mL/min air at 80°C as monitored by TGA.

Computational Studies

An atomic level understanding of carbon capture solvents can provide us further insight of their behavior and can help to design better solvents in the future. In this work, we used computational methods to calculate the partial atomic charges on the O atoms of TBP, T^{i}BP, and (**1**) – (**3**), the interaction energies of these different atom sites with CO_2, and the fractional free volume of these solvents.

Computational calculations were performed to calculate the amount of negative charge on all oxygen atoms in the solvents prepared in this study. Results for all four molecules in this study are shown in Figure 6. These calculations reveal that the highest negative charges were always located on the phosphoryl O, regardless of PEG-arm length or butyl group branching. This negative charge was largest for (**2**) and was smallest for T^{i}BP. The negative charges on the phosphoryl O of all the solvent molecules are very close, and the small differences of charges in molecules (**1**) – (**3**) could be attributed to the vicinity atoms of phosphoryl O in the optimized structures.

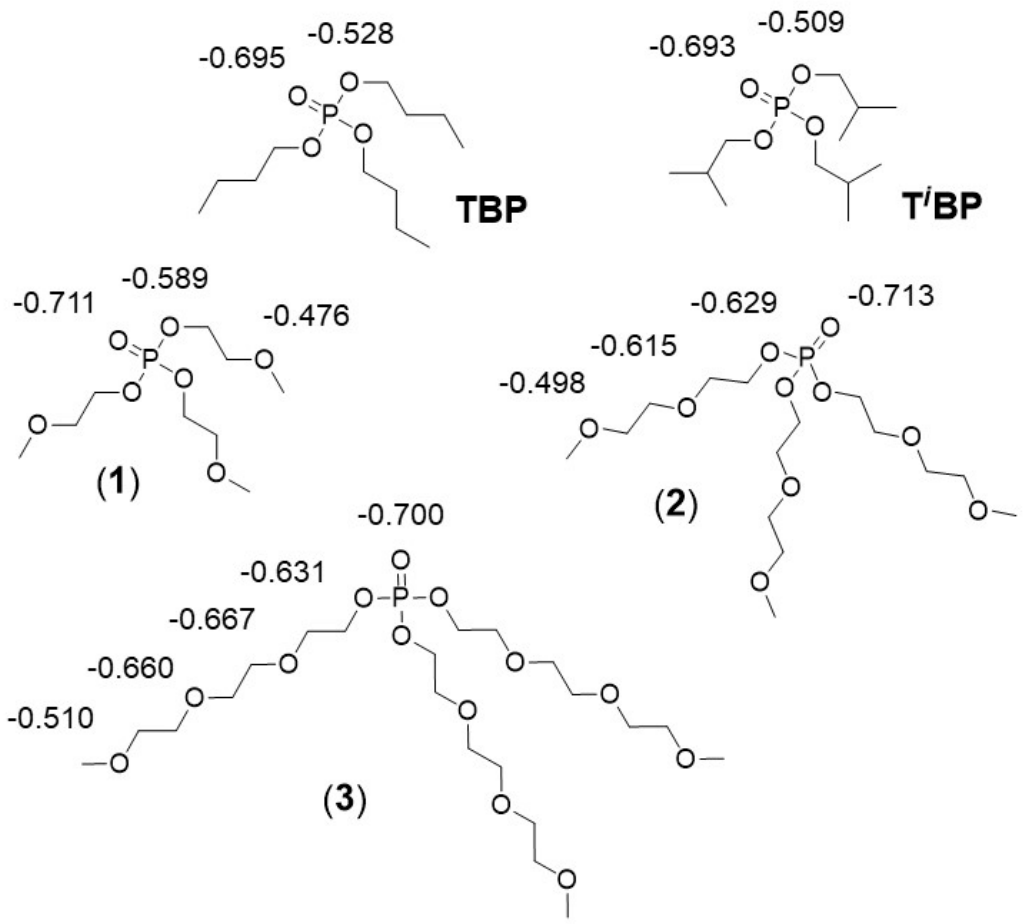

Figure 6. Calculated negative charges on oxygen atoms (**1**) - (**3**), TBP, and T^{i}BP.

The charges on the O atoms in the PEG arms tended to decrease with distance removed from the phosphoryl group. In (**1**) and (**2**) the charges consistently decreased away from the phosphoryl group, whereas in (**3**) they were slightly elevated at the two internal etheric O atoms. For all three phosphate esters, the lowest negative charges for all O atoms in all molecules were consistently located at the terminal methoxy O atom. These results suggest that the phosphoryl group is the most likely location for interaction with CO_2, even when PEG groups are present.

Further results agreed that the location for strongest CO_2 approach was always at the phosphoryl O atom in all five solvents. The CO_2 approach distance at this oxygen atom was always at the shortest distance and the CO_2 interaction energy at this location was always largest. These are shown in Figure 7. CO_2 approach distance and interaction energies were only slightly less favorable at the terminal methoxy O atoms of (**1**) – (**3**) but were significantly less favorable at the internal etheric O atoms. This is likely influenced by the steric bulk of the PEG arms making approach of the internal O atoms by CO_2 more difficult. This also explains why adding etheric groups to TBP fails to improve CO_2 absorption: the primary interaction site is always at the phosphoryl O atom, where the interaction is far stronger than at any ether O atom.

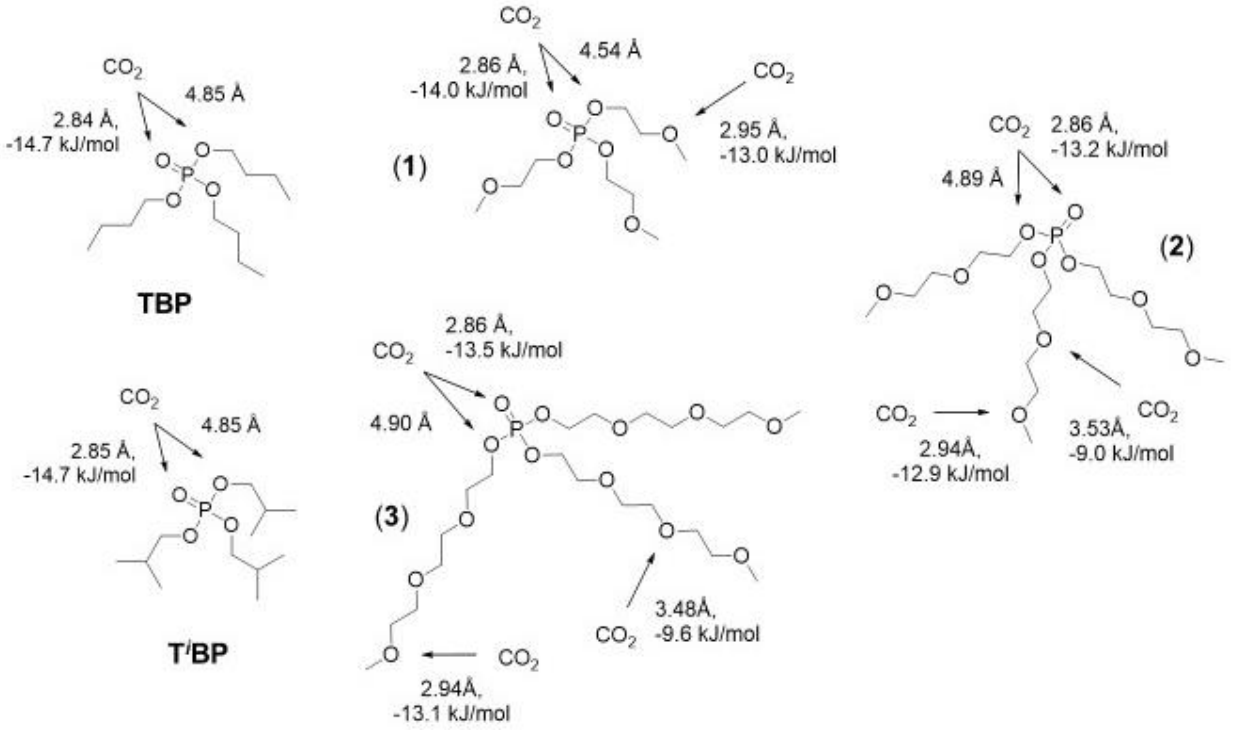

Figure 7. Calculated interaction distances with CO_2 and interaction energies for all oxygen atoms with solvent molecules TBP, T^{i}BP, and (**1**) - (**3**).

It has been suggested by Shi, et al.[30] that it might be preferable, for solvents intended to separate CO_2 from other sparingly soluble gases like H_2, to have low molar volumes, and thus small fractional free volumes (FFV), to minimize the H_2 absorption while still maintaining a sufficiently high CO_2 solubility through chemical interactions with functional groups.[11] Free volume is related to the density and molar volume of the solvent. Computational results for the FFV for each solvent are shown in Table 5. T^{i}BP gave the largest FFV, as would be expected due to the branched nature of the isobutyl groups. The FFV of (**1**) – (**3**) steadily decreased as the PEG arms grew longer. These calculated values were in general agreement with the experimental gas absorption data in Table 3 which shows that the molecules with longer PEG arms absorbed less CO_2 while branched T^{i}BP absorbed slightly more CO_2 than linear TBP. As seen in Figure 8, a plot of the 25°C CO_2 absorption capacity versus solvent FFV showed a linear relationship ($r = 0.9945$), suggesting that FFV is the dominant factor in CO_2 absorption in these solvents. Although introducing PEG groups to these molecules increased the number of interaction sites with CO_2, solvents (**1**) – (**3**) showed poorer CO_2 absorption than TBP and T^{i}BP due to decreased solvent FFV.

Table 5. Calculated solvent FFV for TBP, T^{i}BP, and PEG-substituted organophosphates.

product	**FFV**	**Normalized FFV**[a]
TBP[a]	0.2247	1.000
T^{i}BP	0.2335	1.039
OP(1PEG)$_3$ (**1**)	0.1799	0.800
OP(2PEG)$_3$ (**2**)	0.1644	0.731
OP(3PEG)$_3$ (**3**)	0.1561	0.695

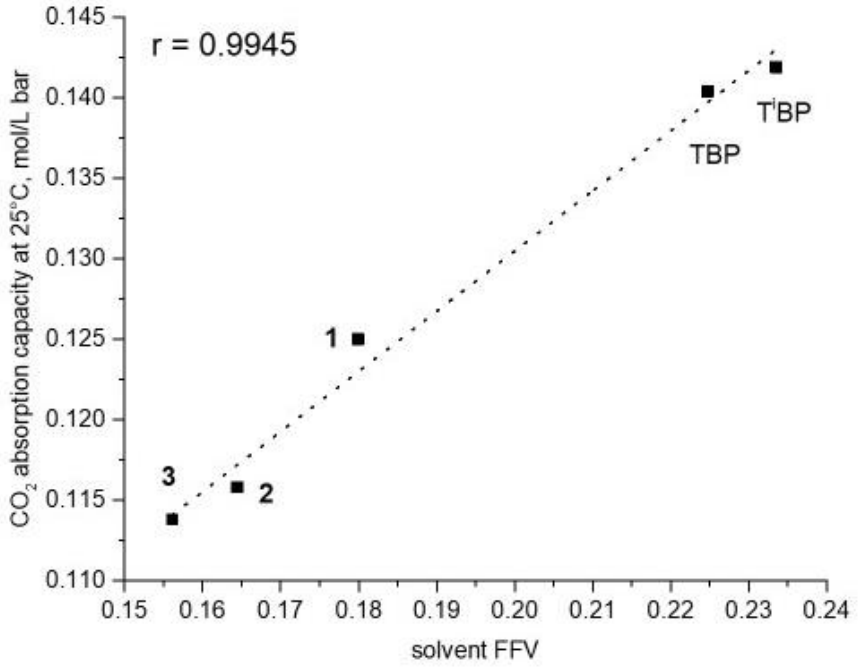

Figure 8. Plot of CO_2 absorption capacity at 25°C versus solvent fractional free volume for (**1**) - (**3**), TBP, and T^{i}BP.

Conclusions

Previous success in improving the usefulness of physical carbon capture solvents by imparting PEG functionality led us to compare TBP, T^{i}BP and three analogous organophosphate solvents in which the length of PEG-substitution was varied. The PEG-substituted solvents (**1**) – (**3**) proved to have acceptable densities and viscosities, but all three solvents showed poorer CO_2 absorption at both 25 and 40°C than TBP or T^{i}BP. Inclusion of hydrophilic PEG groups in solvents (**1**) – (**3**) also led to the undesired absorption of larger amounts of water from humidified N_2 compared to TBP and T^{i}BP. The thermal decomposition temperature of the PEG-substituted solvents increased with increasing molecular weight for all three solvents. Study of the evaporation at 80°C for solvents (**1**) – (**3**) showed them losing significantly less mass than TBP or T^{i}BP.

Computational studies of the analogous organophosphate solvents were performed, calculating partial negative charges as well as CO_2 interaction energies and distances for all O atoms located in these solvents. All five molecules had the lowest partial negative charges, closest CO_2 interaction, and largest CO_2 interaction energy at the phosphoryl O atom. The addition of etheric groups to TBP fails to improve CO_2 absorption because the additional ether groups have CO_2 interactions which are much smaller than with the phosphoryl group. The solvent FFV were computed and was found to be largest for T^{i}BP and grew progressively smaller as the length of the PEG group grew longer in solvents (**1**) – (**3**). It was concluded that FFV was the dominant factor for determining CO_2 absorption ability in organophosphate solvents.

Acknowledgement

This project was funded by the Department of Energy, National Energy Technology Laboratory, an agency of the United States Government under the Carbon Capture field work proposal, and in part through a support contract with Leidos Research Support Team (LRST, contract

89243318CFE000003). Neither the United States Government nor any agency thereof, nor any of their employees, nor LRST, nor any of their employees, makes any warranty, expressed or implied, or assumes any legal liability or responsibility for the accuracy, completeness, or usefulness of any information, apparatus, product, or process disclosed, or represents that its use would not infringe privately owned rights. Reference herein to any specific commercial product, process, or service by trade name, trademark, manufacturer, or otherwise, does not necessarily constitute or imply its endorsement, recommendation, or favoring by the United States Government or any agency thereof. The views and opinions of authors expressed herein do not necessarily state or reflect those of the United States Government or any agency thereof.

References

1. Bucklin, R.W.a.S., R. L.: Comparison of Fluor Solvent and Selexol Processes. Energy Progress **4**(3), 137-142 (1984).
2. Burr, B., Lyddon, L.: Which physical solvent is best for acid gas removal? . Hydrocarbon Processing **88**(1), 43-50 (2009).
3. Kohl, A.L.a.N., Richard B. : Gas Purification, 5th ed. Gulf Professional Publishing, (1997)
4. Gatti, M., Martelli, E., Marechal, F., Consonni, S.: Review, modeling, Heat Integration, and improved schemes of Rectisol (R)-based processes for CO2 capture. Appl. Therm. Eng. **70**(2), 1123-1140 (2014). doi:10.1016/j.applthermaleng.2014.05.001
5. Damen, K., Gnutek, R., Kaptein, J., Nannan, N.R., Oyarzun, B., Trapp, C., Colonna, P., van Dijk, E., Gross, J., Bardow, A.: Developments in the pre-combustion CO2 capture pilot plant at the Buggenum IGCC. In: Gale, J., Hendriks, C., Turkenberg, W. (eds.) 10th International Conference on Greenhouse Gas Control Technologies, vol. 4. Energy Procedia, pp. 1214-1221. Elsevier Science Bv, Amsterdam (2011)
6. Dave, A., Dave, M., Huang, Y., Rezvani, S., Hewitt, N.: Process design for CO2 absorption from syngas using physical solvent DMEPEG. International Journal of Greenhouse Gas Control **49**, 436-448 (2016). doi:10.1016/j.ijggc.2016.03.015
7. Franckowiak, S.a.N., E.: Estasolvan: New Gas Treating Process. Hydrocarbon Processing(May 1970), 145-148 (1970).
8. Renon, H., Lenoir, J.Y., Renault, P.: Gas chromatographic determination of Henry's constants of 12 gases in 19 solvents. Journal of Chemical & Engineering Data **16**(3), 340-342 (1971). doi:10.1021/je60050a014
9. Cooper, D.F., Smith, J.W.: Vapor-liquid equilibrium data for system tri-n-butyl phosphate and sulfur dioxide. Journal of Chemical & Engineering Data **19**(2), 133-136 (1974). doi:10.1021/je60061a017
10. Bara, J.E., Gabriel, C.J., Lessmann, S., Carlisle, T.K., Finotello, A., Gin, D.L., Noble, R.D.: Enhanced CO2 Separation Selectivity in Oligo(ethylene glycol) Functionalized Room-Temperature Ionic Liquids. Industrial & Engineering Chemistry Research **46**(16), 5380-5386 (2007). doi:10.1021/ie070437g
11. Shannon, M.S., Tedstone, J.M., Danielsen, S.P., Hindman, M.S., Bara, J.E.: Properties and Performance of Ether-Functionalized Imidazoles as Physical Solvents for CO2 Separations. Energy & Fuels **27**(6), 3349-3357 (2013). doi:10.1021/ef400362b
12. Shannon, M.S., Bara, J.E.: Properties of Alkylimidazoles as Solvents for CO2 Capture and Comparisons to Imidazolium-Based Ionic Liquids. Industrial & Engineering Chemistry Research **50**(14), 8665-8677 (2011). doi:10.1021/ie200259h
13. Siefert, N.S., Agarwal, S., Shi, F., Shi, W., Roth, E.A., Hopkinson, D., Kusuma, V.A., Thompson, R.L., Luebke, D.R., Nulwala, H.B.: Hydrophobic physical solvents for pre-combustion CO2 capture: Experiments, computational simulations, and techno-economic analysis. International Journal of Greenhouse Gas Control **49**, 364-371 (2016). doi:http://dx.doi.org/10.1016/j.ijggc.2016.03.014
14. Thompson, R.L., Culp, J., Tiwari, S.P., Basha, O., Shi, W., Damodaran, K., Resnik, K., Siefert, N., Hopkinson, D.: Effect of Molecular Structure on the CO2 Separation Properties of Hydrophobic Solvents Consisting of Grafted Poly Ethylene Glycol and Poly Dimethylsiloxane Units. Energy & Fuels **33**(5), 4432-4441 (2019). doi:10.1021/acs.energyfuels.9b00500
15. Hess, A., Barber, G., Chen, C., Mallouk, T.E., Allcock, H.R.: Organophosphates as Solvents for Electrolytes in Electrochemical Devices. ACS Applied Materials & Interfaces **5**(24), 13029-13034 (2013). doi:10.1021/am403924t

16. Morford, R.V., Welna, D.T., Kellam, C.E., Hofmann, M.A., Allcock, H.R.: A phosphate additive for poly(ethylene oxide)-based gel polymer electrolytes. Solid State Ionics **177**(7), 721-726 (2006). doi:http://dx.doi.org/10.1016/j.ssi.2006.01.014
17. Morford, R.V., Kellam, E.C., Hofmann, M.A., Baldwin, R., Allcock, H.R.: A fire-resistant organophosphorus gel polymer electrolyte additive for use in rechargeable lithium batteries. Solid State Ionics **133**(3), 171-177 (2000). doi:http://dx.doi.org/10.1016/S0167-2738(00)00741-4
18. Shiflett, M.B., Yokozeki, A.: Solubility and diffusivity of hydrofluorocarbons in room-temperature ionic liquids. Aiche Journal **52**(3), 1205-1219 (2006). doi:10.1002/aic.10685
19. Shiflett, M.B., Yokozeki, A.: Solubilities and diffusivities of carbon dioxide in ionic liquids: bmim PF6 and bmim BF4. Industrial & Engineering Chemistry Research **44**(12), 4453-4464 (2005). doi:10.1021/ie058003d
20. Shiflett, M.B., Yokozeki, A.: Solubility of CO2 in Room Temperature Ionic Liquid [hmim][Tf2N]. The Journal of Physical Chemistry B **111**(8), 2070-2074 (2007). doi:10.1021/jp067627+
21. Breneman, C.M., Wiberg, K.B.: DETERMINING ATOM-CENTERED MONOPOLES FROM MOLECULAR ELECTROSTATIC POTENTIALS - THE NEED FOR HIGH SAMPLING DENSITY IN FORMAMIDE CONFORMATIONAL-ANALYSIS. J. Comput. Chem. **11**(3), 361-373 (1990). doi:10.1002/jcc.540110311
22. Shi, W., Siefert, N.S., Baled, H.O., Steckel, J.A., Hopkinson, D.P.: Molecular Simulations of the Thermophysical Properties of Polyethylene Glycol Siloxane (PEGS) Solvent for Precombustion CO2 Capture. J. Phys. Chem. C **120**(36), 20158-20169 (2016). doi:10.1021/acs.jpcc.6b06810
23. Shi, W., Myers, C.R., Luebke, D.R., Steckel, J.A., Sorescu, D.C.: Theoretical and experimental studies of CO2 and H2 separation using the 1-ethyl-3-methylimidazolium acetate ([emim][CH3COO]) ionic liquid. J. Phys. Chem. B **116**(1), 283-295 (2012). doi:10.1021/jp205830d
24. M. J. Frisch, G.W.T., H. B. Schlegel, G. E. Scuseria, M. A. Robb, J. R. Cheeseman, G. Scalmani, V. Barone, B. Mennucci, G. A. Petersson, H. Nakatsuji, M. Caricato, X. Li, H. P. Hratchian, A. F. Izmaylov, J. Bloino, G. Zheng, J. L. Sonnenberg, M. Hada, M. Ehara, K. Toyota, R. Fukuda, J. Hasegawa, M. Ishida, T. Nakajima, Y. Honda, O. Kitao, H. Nakai, T. Vreven, J. A. Montgomery, J. E. P. Jr., F. Ogliaro, M. Bearpark, J. J. Heyd, E. Brothers, K. N. Kudin, V. N. Staroverov, R. Kobayashi, J. Normand, K. Raghavachari, A. Rendell, J. C. Burant, S. S. Iyengar, J. Tomasi, M. Cossi, N. Rega, J. M. Millam, M. Klene, J. E. Knox, J. B. Cross, V. Bakken, C. Adamo, J. Jaramillo, R. Gomperts, R. E. Stratmann, O. Yazyev, A. J. Austin, R. Cammi, C. Pomelli, J. W. Ochterski, R. L. Martin, K. Morokuma, V. G. Zakrzewski, G. A. Voth, P. Salvador, J. J. Dannenberg, A. D. S. Dapprich, Ö. Daniels, Farkas, J. B. Foresman, J. V. Ortiz, J. Cioslowski and D. J. Fox: Gaussian 09, Revision A.1. In. Gaussian, Inc., Wallingford, CT, (2009)
25. Zhao, Y.H., Abraham, M.H., Zissimos, A.M.: Fast calculation of van der Waals volume as a sum of atomic and bond contributions and its application to drug compounds. J. Org. Chem. **68**(19), 7368-7373 (2003). doi:10.1021/jo034808o
26. Wagner, E.L.: Calculated Bond Characters in Phosphoryl Compounds. Journal of the American Chemical Society **85**(2), 161-164 (1963). doi:10.1021/ja00885a012
27. Gorenstein, D.G.: Phosphorous-31 NMR: Principles and Applications. Elsevier Science, (2012)
28. Gorenstein, D.G.: Dependence of phosphorus-31 chemical shifts on oxygen-phosphorus-oxygen bond angles in phosphate esters. Journal of the American Chemical Society **97**(4), 898-900 (1975). doi:10.1021/ja00837a039
29. Menger, F.M., Chlebowski, M.E.: Is the ether group hydrophilic or hydrophobic? Langmuir **21**(7), 2689-2695 (2005). doi:10.1021/la040113m
30. Shi, W., Sorescu, D.C., Luebke, D.R., Keller, M.J., Wickramanayake, S.: Molecular Simulations and Experimental Studies of Solubility and Diffusivity for Pure and Mixed Gases of H-2, CO2, and Ar Absorbed in the Ionic Liquid 1-n-Hexyl-3-methylimidazolium Bis(Trifluoromethylsulfonyl)amide (hmim Tf2N). Journal of Physical Chemistry B **114**(19), 6531-6541 (2010). doi:10.1021/jp101897b